



## KKU Engineering Journal

<https://www.tci-thaijo.org/index.php/easr/index>

Published by the Faculty of Engineering, Khon Kaen University, Thailand

### Structural comparison of anodic nanoporous-titania fabricated from single-step and three-step of anodization using a two parallel electrode anodizing cell

Mallika Thabuoat and Chaiyaput Kruehong\*

Department of Chemical Engineering, Faculty of Engineering, KhonKaen University, KhonKaen 40002, Thailand

Received July 2015  
Accepted July 2015

#### Abstract

Anodization of a Ti sheet in an ethylene glycol electrolyte containing 0.38wt%  $\text{NH}_4\text{F}$  with the addition of 1.79wt%  $\text{H}_2\text{O}$  at room temperature was studied. An applied potential of 10-60 V and anodizing time of 1-3 h were used in a single-step and three-step of anodization within a two parallel electrode anodizing cell. Their structural and textural properties were investigated using X-ray diffraction (XRD) and scanning electron microscopy (SEM). After annealing at 600°C in an air furnace for 3 h,  $\text{TiO}_2$ -nanotubes was transformed so that they had a higher proportion of the anatase crystal phase. Also, crystallization of the anatase phase was enhanced as the duration of anodization during the final step was increased. Using a single-step anodization, the pore texture of the oxide film began to appear at an applied potential of 30 V. Increased orderly arrangement of the  $\text{TiO}_2$ -nanotube array with a larger pore size was obtained with increased applied potential. An applied potential of 60 V was selected for the three-step anodization with anodizing times of 1-3 h. The results showed that a smooth surface coverage with a higher density porous- $\text{TiO}_2$  layer was achieved using prolonging times during the first and second steps. However, discontinuity of tubes in length was produced instead of long-vertical tubes. Layer thickness of the anodic oxide film depended on the anodizing time at the last step of anodization. Better arrangement of nanostructured- $\text{TiO}_2$  was produced using a three-step anodization process at 60 V with 3 h for each step.

**Keywords:** Anodization, Anodic titania, Nanotubes, Titanium, Porous structure

#### 1. Introduction

Due to the unique properties of its extremely small size and large surface to volume ratio, nanostructured-titania or titanium dioxide ( $\text{TiO}_2$ ) has attracted great interests in various potential technological applications such as photocatalysts, solar hydrogen generation and gas sensors [1-4]. Different manipulations of the size and shape such as tubes, rods, ribbons, fibers and wires in the nanometer region, were investigated to demonstrate their properties.  $\text{TiO}_2$  can be synthesized via many pathways, for example, the use of nanoporous alumina templates, chemical vapor deposition (CVD), electrochemical anodic oxidation, seeded-growth method, wet chemical (hydrothermal method) and sol gel method.

Among these techniques, electrochemical anodic oxidation or anodization has been received extensive attentions due to controllable, reproducible results as well as its simplest and likely the cheapest one [5-6]. It is a self-assembling process, in which both the localized chemical dissolution and the field assisted oxidation and dissolution lead to the formation of orderly nanotubes [7]. Micropores as well as nanopores with a diameter of several micrometers to a few tens of nanometers can be adjusted by controlling of anodization conditions [8]. The thickness of oxide layer or

nanotube dimensions can be simply controlled by the optimization of various parameters such as pH, concentration and composition of the electrolyte, applied potential, time, and temperature of anodization. The tubes formed in the viscous electrolyte; such as glycerol and ethylene glycol, are entirely smooth (ripple-free) over their entire length [9]. Amount of addition water in this viscous electrolyte has affected on the  $\text{TiO}_2$  structure as the layer exhibits a sponge-like structure when the water content was lower than 1wt%, and the nanotubes formed in the water content of 6wt% showed ridges on the tube wall and the number of the ridges increased with increase in water content [10]. A multi-step anodizing procedure was proposed to obtain high-order of nanopores in the anodic titanium dioxide layer [11-12]. However, none of works have been reported about the properties of nanostructured- $\text{TiO}_2$  fabricated using different approaches for anodization.

In this work, we aimed to investigate the self-organized orderly formation of nanostructured- $\text{TiO}_2$  by anodization of titanium sheet (Ti) in the ethylene glycol-based electrolyte containing of 0.38wt%  $\text{NH}_4\text{F}$  and 1.79wt% water. In particular, the effects of anodizing procedure on structural dimensions and surface morphology of anodic titania were discussed.

\*Corresponding author. Tel.: +66 4336 2240  
Email address: [chai.kr@kku.ac.th](mailto:chai.kr@kku.ac.th)  
doi: 10.14456/kkuenj.2016.3

## 2. Materials and methods

### 2.1 Fabrication of the nanoporous $\text{TiO}_2$

A commercial titanium (Ti) sheet with 99% purity purchased from KVM Heating Element Co., Ltd. (THAILAND) was cut into coupons (2cm x 2cm) with the working area of 1 cm<sup>2</sup>. Prior to anodization, these coupons were degreased ultrasonically in ethanol for 5 min, followed by rinsing with deionized water (DI) and drying in ambient air. Subsequently, the cleaned samples were chemical polished by soaking in a mixture of HF and HNO<sub>3</sub> (25:75 vol%) for 10 s to eliminate the native oxide. An anodization was performed in a two paralleled-electrodes cell under the room temperature, conducted at a constant voltage ranging between 10-60 V for 1-3 h. The same setup of anodizing cell in the previous work was used [13], the titanium coupons were used both as the working electrode and counter electrode and the distance between them was kept at 2 cm. All electrolytes were prepared from reagent grade chemicals and deionized water. Single-step and three-step of anodization were conducted in an ethylene glycol electrolyte containing 0.38wt% NH<sub>4</sub>F with the addition of 1.79wt% water. For the three-step of anodization, an adhesive tape was used to remove the oxide layer which formed during the previous anodizing steps before re-anodized at the next step under the same conditions. After anodization was completed, the samples were taken out from the electrolyte solution immediately and rinsed with distilled water, then dried at ambient atmosphere. Subsequently, the as-synthesized nanoporous  $\text{TiO}_2$  were calcined at 600°C for 3 h with a heating rate of 5°C/min in air.

### 2.2 Characterization of as-formed and annealed nano- $\text{TiO}_2$

The phase purity and crystal structure of the obtained products were examined by XRD using a Philip X' Pert PRO diffractometer (Phillips PW3020) equipped with Cu K $\alpha$  radiation in the 2 $\theta$  range 20–80°, employing a step size of 0.038 using a Cu target at the scan rate of 4 deg/min. The accelerating voltage was set at 40 kV with 40 mA flux. The morphologies of anodic porous  $\text{TiO}_2$  structures were observed with a scanning electron microscope (SEM, S-3000N, Hitachi).

## 3. Results and discussion

Titanium (Ti) specimens were cleaned before anodic oxidation in order to remove the native oxide film, grease and dirt away. This pretreatment was very important step to obtain more desirable anodic  $\text{TiO}_2$  nanotubes with well-vertical alignment [14], since the adhesion between the film and the surface of titanium can be improved. To avoid the corrosion of Ti surface which led to either none oxide coating or the weak adhesion between oxide film and substrate, specimens were soaked into the acid mixture of HF/HNO<sub>3</sub> for a short time of 10 s after washing with ethanol and water. As seen in Figure 1, a clean roughness surface with grains and grain boundaries of Ti sheet was observed after surface pretreatment. The rougher Ti surface provides better adherence of the  $\text{TiO}_2$  nanotube to Ti with uniformly growth of nanotubes underneath the initial porous oxide layer without collapsing behavior [15-16].

As described before [17], the anodization mechanism for creating the nanotube structure was begun with a nano scale  $\text{TiO}_2$  passivation layer on the Ti surface followed by a pit formation on the  $\text{TiO}_2$  layer under the constant applied

potential. As anodization time increases, the pit grows longer and larger, and at last it becomes a nanopore which undergoes continuously through the barrier layer. The completely developed nanotubes are formed on the Ti surface after specific anodization time. As the electrolyte viscosity affects the diffusion of chemical species and formation of the tubes, therefore, the electrochemical anodization of Ti in non-aqueous electrolytes of high viscosity gave the lower degree of local acidification as  $\text{Ti}^0 \rightarrow \text{Ti}^{4+}$  oxidation at the growing tube-tip [18]. Overall results showed that using water-based electrolyte obtained the shorter length tubes with larger diameter and ripples on the tube-walls [9]. The tubes formed in the viscous electrolyte are entirely smooth or ripple-free over their entire length [9, 19]. However, a minimum amount of water addition was required to form the well-ordered  $\text{TiO}_2$  nanotubular arrays [20]. Therefore, this present study used the EG electrolyte containing 0.38wt% NH<sub>4</sub>F with the addition of 1.79wt% H<sub>2</sub>O to fabricate the anodic  $\text{TiO}_2$  film. Since a higher anodization current was obtained at shorter working distance. The temperature of the electrolyte increases gradually during the anodization and so the mobility of ions in electrolyte increases, giving a larger pore diameter [21]. So the distance between electrodes was fixed at 2 cm, and the anodization was investigated at the room temperature.

### 3.1 Effect of applied potential and anodizing time on the morphology of anodic $\text{TiO}_2$ film produced by single-step of anodization

From single step of anodization for 1 h, it was found that using low voltage of 10 V presented a non-uniform surface covered by a thin oxide (Figure 2a). More nonporous film was accumulated at the higher applied potential of 30 V (Figure 2b), the surface of the grains and grain boundaries are covered with an irregular porous oxide. Anodization at 40 V provided more uniform distribution of porous oxide surface covered each individual grain which was separated by the obviously grain (Figure 2c). The oxide dissolution at the grain boundaries was accelerated by the void defects. Each grain was filled with higher consistency of porous oxide due to the forming rate resulted by the oxidation reaction that might be a slightly greater than the dissolution rate. However, anodization of Ti sheet at higher potential of 60 V, the top surface of porous oxide was connected into the small clusters as seen in Figure 2d. The obvious dissolution of the surface oxide took place and some nanotubes overlapped each other due to the accelerated reaction between  $\text{TiO}_2$  and F<sup>-</sup> concentrations under high voltage.

The anodizing time is also the key factor determining the nanotube length as the tube length increases with increasing of anodization duration [10]. In this study, anodizing time was increased to 3 h under the same anodizing conditions applied to 1 h of anodization. Results showed not only the density of porous oxide was increased with the intensity of applied potential but also the trend of oxide formation was similar presented to the anodic film produced at 1 h of anodization. At low voltages of 10 V and 20 V, the surface was covered by nonporous oxide layer intensively as seen in Figure 3a and 3b, respectively. The porous oxide surface with the top oxide structured like rod or needle bar started to reveal after anodization at the higher potential of 30 V (Figure 3c) because of the localized different rates between formation and dissolution. Higher level of nanoporous surface increased with the applied voltage of 40 V (Figure 3d). Same result to the single anodization for 1 h was

revealed as each grain was uniformly covered by the porous oxide with the dominant separation among grain boundaries. With the applied potential of 50 V (Figure 3e), grain surfaces had more smooth consistency of porous oxide. All grain boundaries were fulfilled with oxide due to the forming rate is slightly greater than the dissolution rate as similar explanation in the results from the single anodization for 1 h. However, when using high voltage of 60 V (Figure 3f), the whole surface was not covered by porous oxide resulted from the faster reaction between  $\text{TiO}_2$  and F<sup>-</sup> under the high voltage intensity and prolonging time of anodization. Moreover, the thickness of oxide layer increased with the increase in applied potential and anodizing time as illustrated in Figure 4. The oxide layer grows rapidly at the higher applied potential because the flowing current is relatively

high, these results were consistent with elsewhere reports [11, 15, 21].

### 3.2 Effect of applied potential and anodizing time on the morphology of anodic $\text{TiO}_2$ film produced by three-step of anodization

To achieve the high-ordered arrangement of nanoporous  $\text{TiO}_2$  layer, a multi-step anodizing procedure was employed at the constant applied potential and then the grown oxide layer was removed before final anodizing step. It had been reported that increasing number of anodizing step gave the pore formation at the steady-state within a shorter time period and higher recorded current densities indicating the nucleation of pores is easier on pre-textured titanium surface [11].

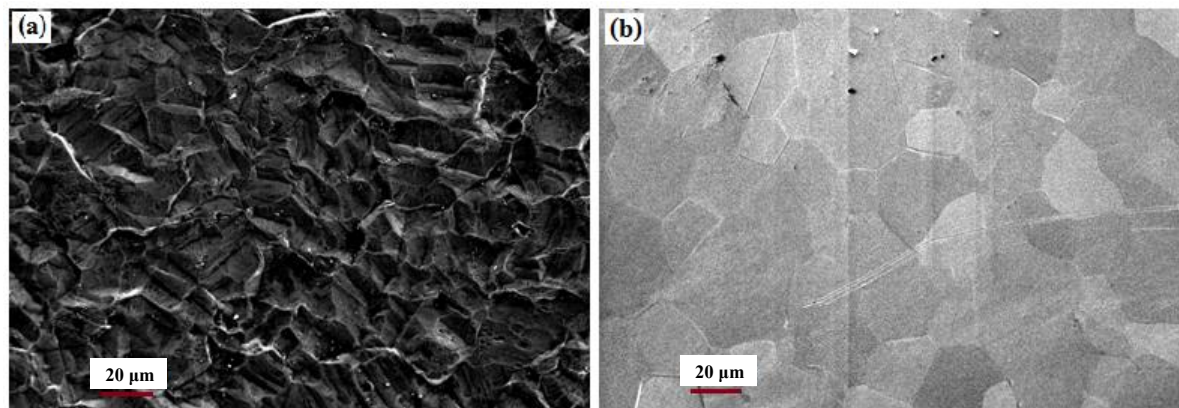


**Figure 1** SEM images of (a) untreated Ti-sheet and (b) cleaned Ti-sheet at 500x magnification.

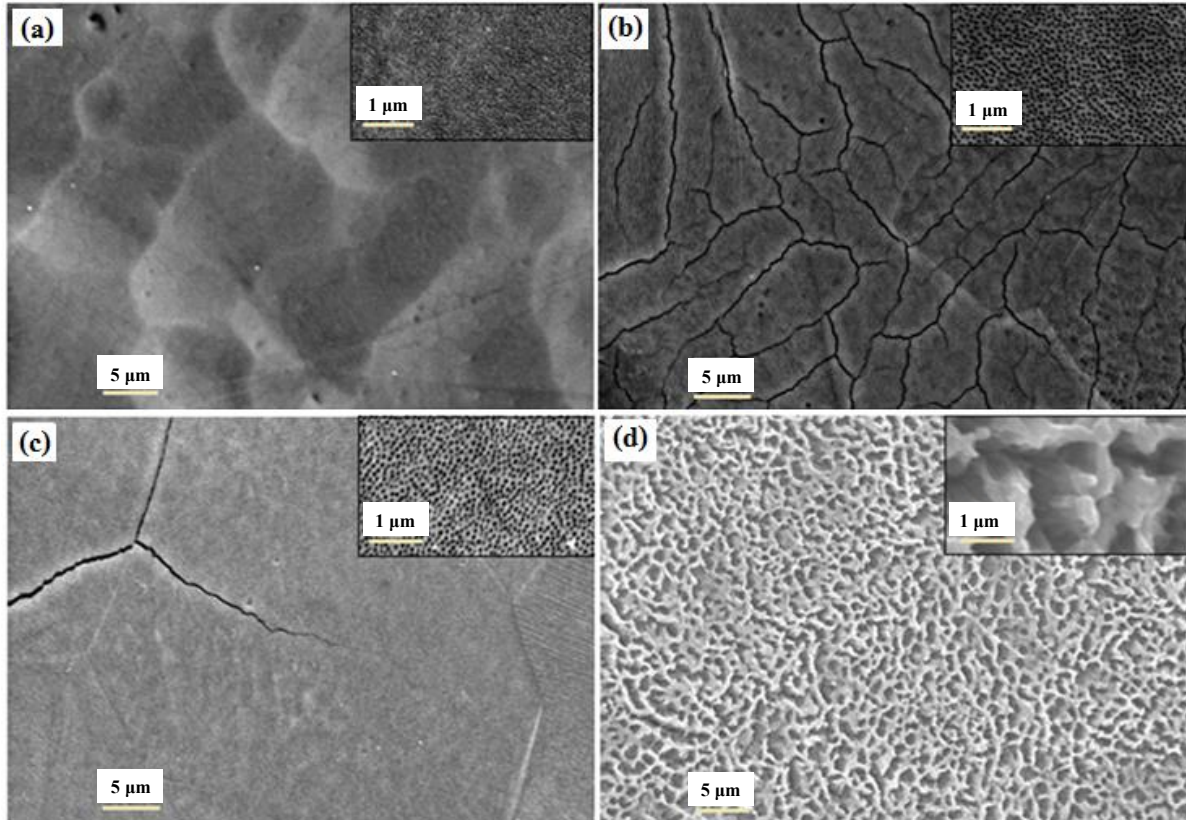


**Figure 2** SEM images at a magnification of 2,000x showing  $\text{TiO}_2$  nanoporous layers grown by single-step of anodization processes of Ti for 1 h (The inset micrographs are at a magnification of 10,000x) under the applied potential of (a) 30V (b) 40V (c) 50V and (d) 60V.



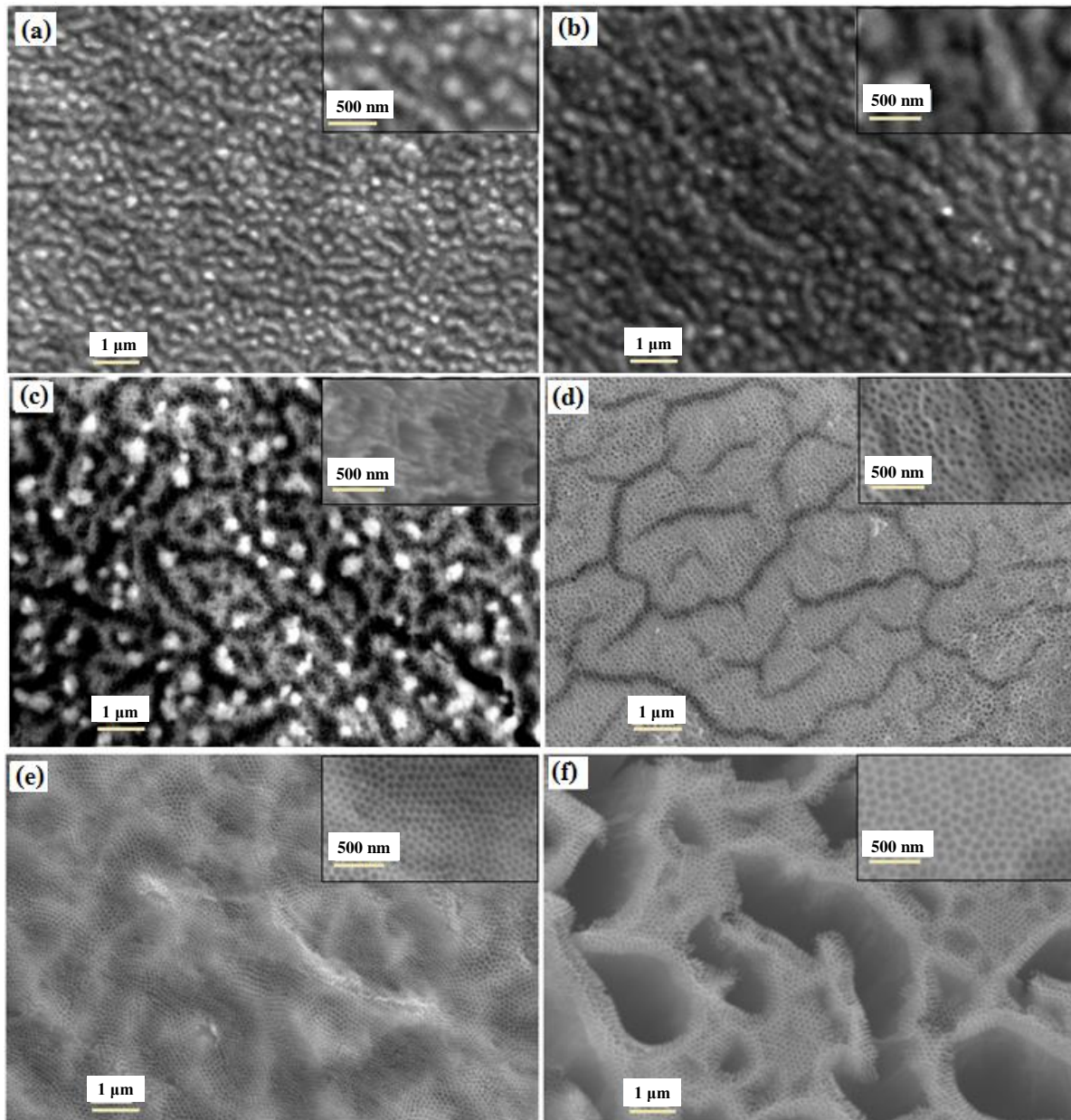


**Figure 3** SEM images at a magnification of 10,000x showing  $\text{TiO}_2$  nanoporous layers grown by single-step of anodization processes of Ti for 3 h (The inset micrographs are at a magnification of 20,000x) under the applied potential of (a) 10 V (b) 20 V (c) 30 V (d) 40 V (e) 50 V and (f) 60V.

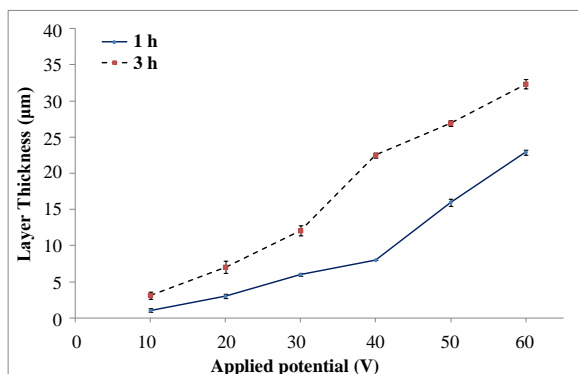


**Figure 4** Layer thickness of  $\text{TiO}_2$  nanotube arrays prepared at different anodizing times as a function of applied potential.

It was found from the single-step of anodization that using 60 V gave the maximum thickness formed  $\text{TiO}_2$  layer even the whole surface was not covered. So the applied potential of 60 V was selected for  $\text{TiO}_2$  preparation via three-step of anodization. As stated in the section of film fabrication, the grown oxide layer after the 1<sup>st</sup> and 2<sup>nd</sup> steps were removed before immediate re-anodization the Ti-substrate under the identical anodizing condition in the previous step. Figure 5 shows the characteristic of  $\text{TiO}_2$  nanotube fabricated on Ti substrate, single-step of anodization gave the well-ordered morphology of  $\text{TiO}_2$  nanotube after reaching the steady-state formation and dissolution of oxide film. For the multi-step of anodization, the regular array of periodic concave formed on the Ti surface after the oxide layer produced from the previous step had been removed. These serve as the nucleation sites for the formation of nanopores in the next anodizing step as discussed in the other literatures

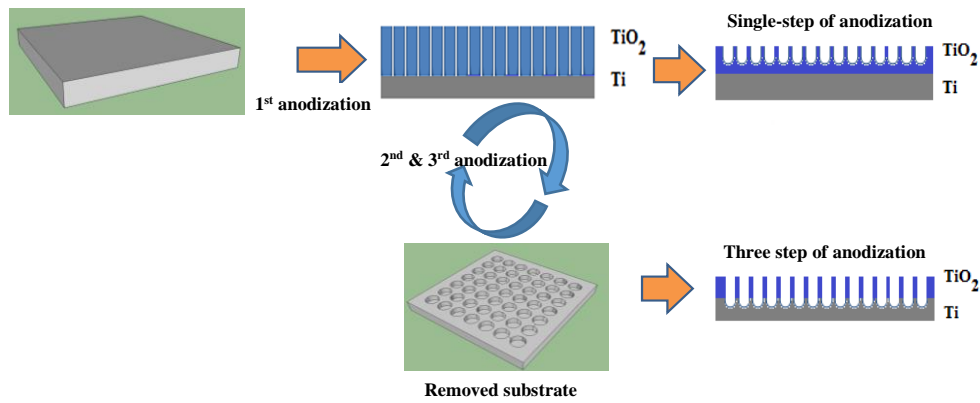


**Figure 5** Schematic representation of fabrication process of obtaining TiO<sub>2</sub> nanotube via single-step and three-step of anodization.

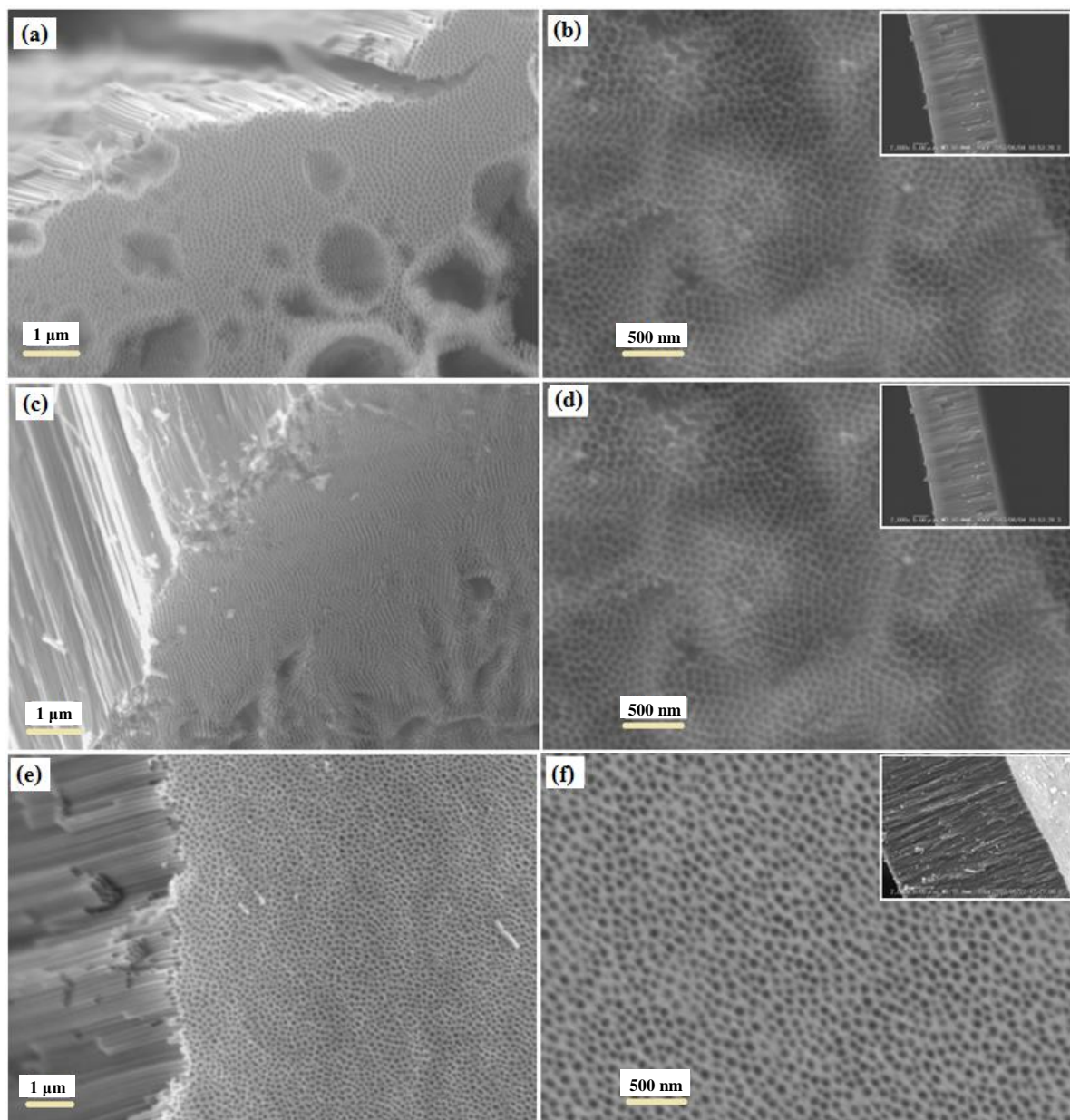


**Figure 6** SEM images showing TiO<sub>2</sub> nanoporous layers grown by three-step of anodization processes of Ti (left side-images and right top-images are at a magnification of 10,000x and 20,000x, respectively) under the applied potential of 60 V under the condition of (a, b) 331 (c, d) 332 and (e, f) 333. The inset micrographs show whole nanotube length.

[11, 22-23]. Therefore, the better vertical arrangement of TiO<sub>2</sub> nanotubes with less thickness of bottom barrier layer and strong adherence on Ti substrate were achieved after the 3<sup>rd</sup> anodization.

Herein, the duration of each anodizing step had contributed to the formation of the TiO<sub>2</sub> film, the anodizing condition was signed as xyz in the meaning that the duration for the 1<sup>st</sup>, 2<sup>nd</sup> and 3<sup>rd</sup> anodization was x, y and z h, respectively. To confirm the influence of the anodizing time, the two former steps were completed with 3 h of each step before re-anodization at the final step with the use of the identical anodizing conditions. Using 331 obtained the concave oxide surface covered on Ti substrate (Figure 6a and 6b). Increasing the time duration for the final anodization as the condition of 332 and 333 obtained more smooth oxide surface (Figure 6c-6f). Especially, well-organized layer of nanotube was presented from anodization using condition of 333. Also, the thickness of the oxide layer increases with the duration of the last anodization step. By the use of conditions 331 332 and 333, the layer thickness were 18, 20 and 40  $\mu\text{m}$ , respectively (Figure 6b, 6d and 6f), however the tube length was discontinued instead of the smooth tube. It could be confirmed that Ti substrate was appropriately supported the formation of TiO<sub>2</sub> nanotubes and prolonging time of anodization increased the growth of oxide layer.

In order to compare the characteristic parameters of porous anodic TiO<sub>2</sub>, the pore shapes were assumed to be the perfect circles as shown in Figure 7. The pore diameter ( $D_p$ ), inter pore distance ( $D_c$ ) and wall thickness ( $W_t$ ) were controlled by anodizing conditions. The average pore diameter and average inter pore distance of each prepared anodic TiO<sub>2</sub> were mathematically calculated from the pore measurement of top-view images which presented in Figure 6b, 6d and 6f. The wall thickness was half-difference between the  $D_c$  and  $D_p$ . The influence of the applied potential on these parameters the anodic nanotubes TiO<sub>2</sub> are presented in Figure 8, the values of  $D_c$ ,  $D_p$  and nanotube length obviously increased with the higher intensity of applied potential and longer anodizing time. Increasing applied potential caused to be higher charged in the anodizing system. After 3 h of anodization, the pore diameter, inter pore distance and nanotube length increased from 61 to 105 nm, 91 to 139 nm and 31 to 40  $\mu\text{m}$ , respectively when anodizing potential increased from 40 to 60 V. For 1 h of anodization, the wall thickness increased with the increase in potential level. While the nanotube TiO<sub>2</sub> with the thinner wall thickness was given from the longer anodizing time of 3 h. These results were in agreement with the other reports [10-11, 15, 17, 21].

### 3.3 Effect of applied potential and anodizing time on the crystalline structure of anodic TiO<sub>2</sub> film produced by three-step of anodization

It was found that the formation of TiO<sub>2</sub> crystallites and enhancement of crystallization was greater with increasing calcination temperatures from 300 to 600°C [24]. For this study, the morphology of TiO<sub>2</sub> nanotubes was changed from amorphous to crystalline (either in the form of anatase or rutile) after calcinations at 600°C for 3 h in the air atmosphere. XRD spectras of prepared samples are presented in Figure 9, peaks of titanium metal, rutile and anatase were depicted as Ti, R and A. The crystalline rutile plane (101) are shown at the diffraction angle of  $2\theta = 36^\circ$ , while the diffraction angles of  $2\theta = 25.3^\circ, 37.22^\circ, 37.8^\circ, 48.1^\circ, 53.3^\circ$  and  $54.46^\circ$  represented the crystalline anatase planes of (101), (004), (002), (200), (105) and (211), respectively. By

using this XRD data, the ratio of the intensity of the anatase or rutile reflections to the intensity of whole crystalline reflections was calculated. The proportion of crystalline anatase was greater than that of crystalline rutile, and it increased from 84.88 to 89.05% when the period of anodization increased from 1 to 3 h.

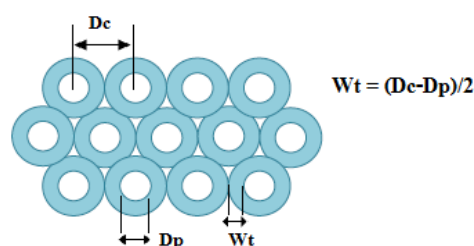


**Figure 7** Schematic representation of the TiO<sub>2</sub> nanoporous structure based on the assumption of completed circle of pore shape.

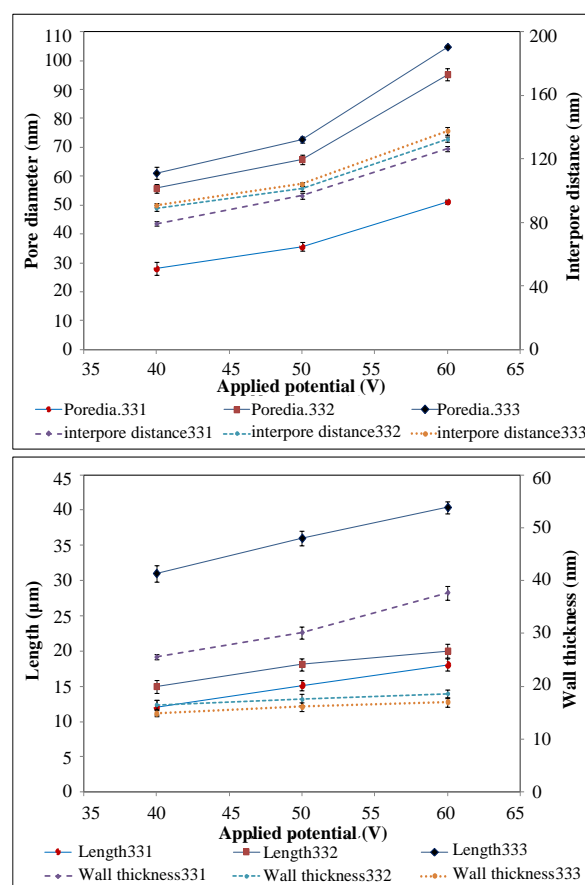


**Figure 8** Effect of anodizing potential on (a) the thickness and inter pore distance, (b) the length and wall thickness, of TiO<sub>2</sub> nanotube layer grown after the third anodization carried out in an ethylene glycol solution containing NH<sub>4</sub>F (0.38wt.%) and H<sub>2</sub>O (1.79wt.%) under 60 V.

## 4. Conclusions

From this study, the single-step of anodization of titanium (Ti) in an ethylene glycol solution containing NH<sub>4</sub>F (0.38wt%) and H<sub>2</sub>O (1.79wt%) under 50 V for 3 h resulted in the satisfied smooth surface coverage with nanoporous TiO<sub>2</sub> film. Its layer thickness increased with the increase of



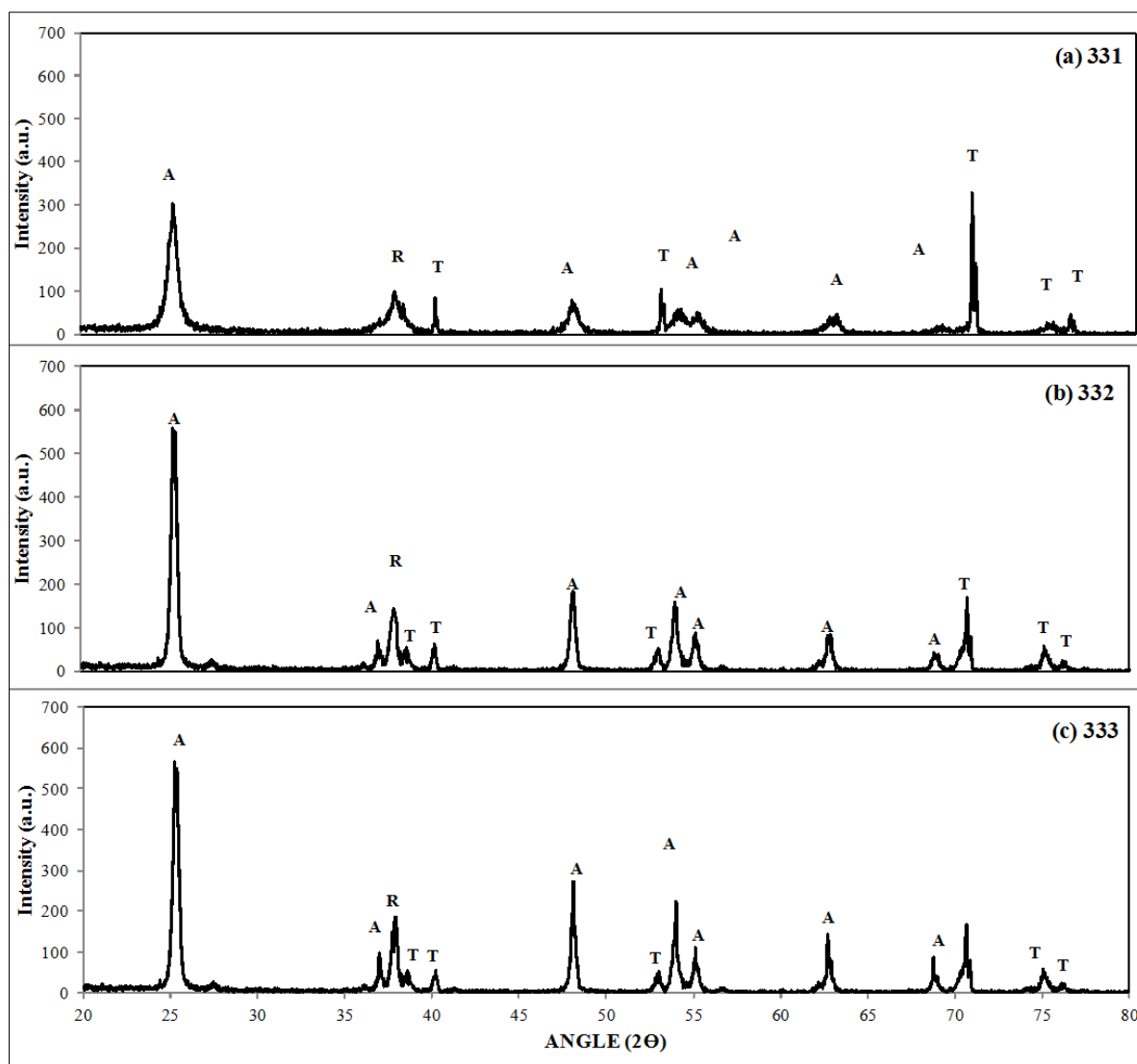


**Figure 9** XRD spectra of TiO<sub>2</sub> nanotubes on Ti substrate prepared using three-step of anodization after annealing at 600°C for 3 h. (A, T and R represents anatase, titanium and rutile, respectively).

potential intensity and anodizing duration. The three-step of anodization of titanium (Ti) in the same electrolyte under 60 V for 3 h of each step resulted in the better-coverage over whole surface with 40  $\mu\text{m}$  maximum length of nanotube-TiO<sub>2</sub>. As the potential intensity and anodizing time increase for the last step, pore diameter, interpore distance, nanotube length and wall thickness increased. Moreover, the maximum anatase content of 89.05% was obtained from the three-step of anodization of titanium in the same electrolyte under 60 V for 3 h of each step.

## 5. Acknowledgements

We are grateful to the PhD scholarship for senior staff affiliated with KhonKaen University, Fiscal year of 2012 for financial support throughout the curriculum.

## 6. References

- [1] Varghese OK, Paulose M, LaTempa TJ, Grimes CA. High-rate solar photocatalytic conversion of CO<sub>2</sub> and water vapor to hydrocarbon fuels. *Nano Lett.* 2009;9(2):731-7.
- [2] Zhao G, Cui X, Liu M, Li P, Zhang Y, Cao T, et al. Electrochemical degradation of refractory pollutant using a novel microstructured TiO<sub>2</sub> nanotubes/Sb-doped SnO<sub>2</sub> electrode. *Environ Sci Tech.* 2009;43(5):1480-6.
- [3] Liu Z, Zhang X, Nishimoto S, Murakami T, Fujishima A. Efficient photocatalytic degradation of gaseous acetaldehyde by highly ordered TiO<sub>2</sub> nanotube arrays. *Environ Sci Tech.* 2008;42(22): 8547-51.
- [4] Zhang Y, Fu W, Yang H, Qi Q, Zeng Y, Zhang T, et al. Synthesis and characterization of TiO<sub>2</sub> nanotubes for humidity sensing. *Appl Surf Sci.* 2008;254(17): 5545-7.
- [5] Zhu X, Chen J, Scheideler L, Reichl R, Geis-Gerstorfer J. Effects of topography and composition of titanium surface oxides on osteoblast responses. *Biomaterials.* 2004;25(18):4087-103.
- [6] Yang B, Uchida M, Kim HM, Zhang X, Kokubo T. Preparation of bioactive titanium metal via anodic oxidation treatment. *Biomaterials.* 2004;25(6):1003-10.

- [7] Rani S, Roy SC, Paulose M, Varghese OK, Mor GK, Kim S, Yoriya S, et al. Synthesis and applications of electrochemically self-assembled titania nanotube arrays. *Phys Chem Chem Phys*. 2010;12(12):2780-800.
- [8] Macák JM, Tsuchiya H, Schmuki P. High-Aspect-Ratio TiO<sub>2</sub> nanotubes by anodization of titanium. *Angew Chem Int Ed*. 2005;44(14):2100-2.
- [9] Macak JM, Schmuki P. Anodic growth of self-organized anodic TiO<sub>2</sub> nanotubes in viscous electrolytes. *Electrochim Acta*. 2006;52(3):1258-64.
- [10] Lin CJ, Yu YH, Chen SY, Liou YH. Anodic growth of highly ordered titanium oxide nanotube arrays: Effects of critical anodization factors on their photocatalytic activity. *World Acad Sci Eng Technol*. 2010;65:1094-9.
- [11] Sulka GD, Kapusta-Kołodziej J, Brzózka A, Jaskuła M. Fabrication of nanoporous TiO<sub>2</sub> by electrochemical anodization. *Electrochim Acta*. 2010;55(14):4359-67.
- [12] Ali G, Chen C, Yoo SH, Kum JM, Cho SO. Fabrication of complete titania nanoporous structures via electrochemical anodization of Ti. *Nanoscale Res Lett*. 2011;6(1):1-10.
- [13] Mallika T, Chaiyaput K. DSSCs fabrication using nano-structured titania as photoanode. *Appl Mech Mater*. 2015;781:184-8.
- [14] Sklar GP, Singh H, Mahajan V, Gorhe D, Namjoshi SA, LaCombe JC. Nanoporous titanium oxide morphologies produced by anodizing of titanium. *Mater Res Soc Symp Proc*. 2005;876:1-6.
- [15] Albu SP. Morphology and Growth of Titania Nanotubes: Nanostructuring and Applications [dissertation]. Erlangen: Universitätsbibliothek Erlangen-Nürnberg; 2012.
- [16] Wu HP, Li LL, Chen CC, Diau EWG. Anodic TiO<sub>2</sub> nanotube arrays for dye-sensitized solar cells characterized by electrochemical impedance spectroscopy. *Ceram Int*. 2012;38(8): 6253-66.
- [17] Brammer KS, Frandsen CJ, Oh S, Jin S. Biomaterials and biotechnology schemes utilizing TiO<sub>2</sub> nanotube arrays. In: Pignatello R, editor. *Biomaterial science and engineering*. Rijeka: INTECH Open Access Publisher; 2011. p. 193-210.
- [18] Nguyen QA, Bhargava YV, Devine TM. Titania nanotube formation in chloride and bromide containing electrolytes. *Electrochem Comm*. 2008;10(3):471-5.
- [19] Macak JM, Tsuchiya H, Taveira L, Aldabergerova S, Schmuki P. Smooth anodic TiO<sub>2</sub> nanotubes. *Angew Chem Int Ed*. 2005;44(45):7463-5.
- [20] Raja KS, Gandhi T, Misra M. Effect of water content of ethylene glycol as electrolyte for synthesis of ordered titania nanotubes. *Electrochem Comm*. 2007;9(5):1069-76.
- [21] Sun L, Zhang S, Sun XW, He X. Effect of electric field strength on the length of anodized titania nanotube arrays. *J Electroanal Chem*. 2009;637(1):6-12.
- [22] Chen J, Lin J, Chen X. Self-assembled TiO<sub>2</sub> nanotube arrays with U-shaped profile by controlling anodization temperature. *J Nanomaterials*. 2010;2010: 1-4.
- [23] Sulka GD, Stępniewski WJ. Structural features of self-organized nanopore arrays formed by anodization of aluminum in oxalic acid at relatively high temperatures. *Electrochim Acta*. 2009;54(14):3683-91.
- [24] Yu J, Wang B. Effect of calcination temperature on morphology and photo-electrochemical properties of anodized titanium dioxide nanotube arrays. *Appl Catal B Environ*. 2010;94(3):295-302.